

## Unusual Phase Separation in a Polymer Solution Caused by Asymmetric Molecular Dynamics

Hajime Tanaka

*Institute of Industrial Science, University of Tokyo, Minato-ku, Tokyo 106, Japan*

(Received 1 February 1993)

Here we demonstrate the first evidence that phase separation in polymer solutions could be essentially different from that in binary liquid systems. This difference is likely to originate from the strong asymmetry in molecular dynamics between the two separated phases. When the rheological time of the polymer-rich phase is slower than the deformation time, the stress field can be strongly coupled with the concentration diffusion and the coarsening dynamics is dominated by the viscoelastic effect. This causes mechanically dominated pattern evolution. The *dynamic symmetry* should be considered in addition to the static, composition symmetry.

PACS numbers: 64.75.+g, 05.70.Fh, 61.25.Hq, 61.41.+e

Polymer solutions and mixtures have so far been believed to belong to the same dynamic universality class as binary liquid mixtures [1], which is known as *model H* in the Hohenberg-Halperin notation [2]. Thus it has commonly been thought that there is nothing special to polymers about phase separation, especially in the late stage [1]. The only exception has so far been the entropy-induced slowing down of coarsening which was shown to be characteristic of phase separation in polymer blends by Kotnis and Muthukumar [3]. All the existing theories assume that the elementary molecular dynamics is much faster than the coarsening dynamics, or the diffusion process is the limiting process. This assumption could be violated when there is a strong *asymmetry in elementary molecular dynamics* between the two components: For a dynamically symmetric case, diffusion always becomes the slowest dynamic process, while for a dynamically asymmetric case it is not necessarily the slowest one. In this Letter we will demonstrate the first experimental evidence that the asymmetry in elementary molecular dynamics plays a crucial role in phase separation.

The coupling between the stress field and the diffusion was first noticed and studied by Brochard and de Gennes [4] for polymer solutions. The problem has recently been extensively studied by many researchers in connection with shear-induced phase separation from theoretical viewpoints [5-7]. Recently Doi and Onuki [7] have derived general diffusion equations including the dynamic coupling between stress and composition, on the basis of the two fluid model. The viscoelastic effect on diffusion and the response to weak shear has mainly been argued [7]. The discussion has mostly been limited to the near-equilibrium state and thus the viscoelastic effect on spinodal decomposition has so far been unexplored. However, we believe the basic idea can be applied for the unstable state far from equilibrium. The polymer composition  $\phi$  probably obeys the following kinetic equations [7]:

$$\frac{\partial \phi}{\partial t} = -\nabla \cdot (\phi v) + \nabla \cdot \frac{\phi^2(1-\phi)^2}{\zeta} \left( \nabla \frac{\delta F}{\delta \phi} - \frac{\nabla \cdot \sigma^{(n)}}{\phi} \right),$$

$$v_p - v_s = -\frac{1-\phi}{\zeta} \nabla \cdot (\pi \mathbf{I} - \sigma^{(n)}),$$

$$\rho_0 \frac{\partial v}{\partial t} = \nabla \cdot [-(\pi + p)\mathbf{I} + \sigma^{(n)}] + \eta_0 \nabla^2 v.$$

Here  $v_p(\mathbf{r}, t)$  and  $v_s(\mathbf{r}, t)$  are the average velocities of polymer and solvent at point  $\mathbf{r}$  and time  $t$ , and  $v = \phi v_p + (1-\phi)v_s$ .  $\phi(\mathbf{r}, t)$  is the composition of polymer.  $\rho_0$  is the average density,  $p$  is the pressure, and  $\zeta$  is the friction constant per unit volume. The free energy  $F$  is given by the following Flory-Huggins-de Gennes form:

$$F = \int d\mathbf{r} [f(\phi) + (K/2)(\nabla \phi)^2],$$

$$f(\phi) = k_B T [(1/N)\phi \ln \phi + (\frac{1}{2} - \chi)\phi^2 + \frac{1}{6}\phi^3 + \dots],$$

where  $N$  is the degree of polymerization and  $\chi$  is the interaction parameter. In the linear response regime  $\sigma^{(n)}$  is generally written as

$$\sigma_{ij}^{(n)} = \int_{-\infty}^t dt' G(t-t') \left[ \frac{\partial v_{pj}}{\partial x_i} + \frac{\partial v_{pi}}{\partial x_j} - \frac{2}{3} (\nabla \cdot v_p) \delta_{ij} \right],$$

where the stress relaxation function  $G(t)$  is related to the complex shear viscosity  $\eta^*(\omega)$  by  $\eta^*(\omega) = \int_0^\infty dt e^{-i\omega t} G(t)$ . The above equations naturally coincide with the equations for hydrodynamic systems if we put  $\nabla \cdot \sigma^{(n)} = 0$ . Here it should be stressed that  $G(t)$  is strongly dependent on  $\phi(\mathbf{r}, t)$  and  $N$ , although it is not explicitly written in the equations. This fact should play a crucial role in the phase-separation dynamics as will be discussed later. Before discussing the viscoelastic effect in unstable states, the experimental evidences indicating the effect will be shown below.

The systems studied were the mixtures of monodisperse polystyrene (PS) and diethyl malonate (DEM). The weight-average molecular weight ( $M_w$ ) of PS, its molecular weight distribution ( $M_w/M_n$ ,  $M_n$ : number-average molecular weight), and the critical composition ( $\phi_c$ ) and temperature ( $T_c$ ) of the mixture are listed in Table I. These mixtures have upper-critical-solution-temperature (UCST) type phase diagrams [8]. The mixtures were sandwiched between two glass plates with a gap of a

TABLE I. Physical characteristics of polymer solutions.

PS	$M_w(10^5)$	$M_w/M_n$	$\phi_c$ (wt. % PS)	$T_c$ ( $^{\circ}\text{C}$ )
PS-L	1.80	1.06	8.7	15.8
PS-M	3.55	1.02	7.0	21.0
PS-H	12.6	1.05	4.0	28.8

few  $\mu\text{m}$ . The phase-separation process was observed with phase contrast microscopy. The quench was accomplished within a few seconds.

Figure 1 shows a schematic phase diagram of polymer solution. Figures 2(a) and 2(b) show the phase-separation behavior observed in PS-H/DEM (0.98 wt. % PS) at  $27.4^{\circ}\text{C}$ . First small droplets of dense polymer phase are formed quickly. These droplets vigorously move around by Brownian motion. Although they have a lot of chance of collisions, the droplet coalescence is rather rare. Thus the system very slowly coarsens with time. The coarsening process was analyzed by digital image analysis (DIA) [9]. The temporal change of the structure factor  $S(q, t)$  calculated by DIA is shown in Fig. 2(c). In this case, we find unusually slow coarsening approximated by  $q_m \sim t^{-\alpha}$  ( $\alpha \sim 0.1$ ), where  $q_m$  is the peak wave number of  $S(q, t)$ . Further, the coarsening rate, i.e., the value of  $\alpha$ , decreases with an increase in the quench depth  $\Delta T$ . This is also different from usual phase separation. The behavior is very similar to the moving droplet phase (MDP) found in a polymer/water mixture having a double-well-shaped phase diagram [10].

Figures 3(A)–3(C) show the phase-separation behavior observed in (1) PS-L/DEM (8.7 wt. % PS), (2) PS-M/DEM (7.0 wt. % PS), and (3) PS-H/DEM (4.0 wt. % PS), respectively. The final value of  $\phi_{\text{pr}}$  ( $\phi_{\text{pr}}$ :  $\phi$  of the polymer-rich phase) for the mixtures (1)–(3) are  $\sim 1.5\phi_c$ ,  $3.3\phi_c$ , and  $4.5\phi_c$ , respectively (see Table I for the val-

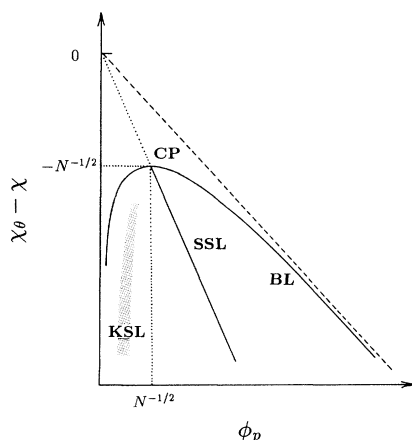


FIG. 1. Schematic phase diagram of a polymer/liquid mixture.  $\chi_{\theta}$  is  $\chi$  at the  $\theta$  temperature and equal to  $1/2$ . BL and CP stand for the binodal line and the critical point, respectively. KSL and SSL indicate the *kinetic-* and *static-symmetry* lines, respectively.

ues of  $\phi_c$ ). Here it should be noted that  $\phi_c$  is close to the chain overlapping concentration  $\phi^*$  and thus the ratio  $\phi_{\text{pr}}/\phi_c$  is directly correlated to the degree of entanglement. In case (1), we see usual pattern evolution characteristic of phase separation in nearly symmetric binary fluid mixtures. The initial interconnected structure transforms into droplet pattern because of a slight asymmetry. In case (2), unusual *networklike pattern* (NP) is seen in the initial stage, but it gradually relaxes to the pattern with round interface in the late stage. In case (3), NP can be seen more clearly. NP looks similar to that observed in Ref. [10]. For both (2) and (3), a very fine structure appears in the initial stage; after a certain incubation time the solvent-rich droplets having a bright contrast emerge, and then grow with time. The apparent volume of the polymer-rich matrix phase keeps decreasing with time [11]. This indicates the temporal change in the concentration distribution even after the formation of sharp interface. This is inconsistent with the conventional picture that the concentration is almost constant with time in the late stage [1]. The coarsening process is characterized by the thinning of the polymer-rich, networklike phase, which is driven by the tension along the thin part. In the final stage, we see the gradual transition from the regime dominated by viscoelasticity to the regime dominated by interfacial tension [see Fig. 3(B)].

In Fig. 4 we show the temporal change in  $q_m$  and  $S(q_m)$  calculated by DIA for the case (3) [see Fig. 3(C)]. There is almost no coarsening until  $t \sim 20$  s and then after the transitional regime from 20 s to 100 s the domains grow as  $q_m \sim t^{-0.15}$ . This initial regime without coarsening (*frozen regime*) is very unusual and characteristic of *viscoelastic spinodal decomposition*. The same exponent ( $\alpha \sim 0.15$ ) in the *growth regime* was commonly observed for Fig. 3(B) and other cases.

The difference in the pattern evolution among Figs.

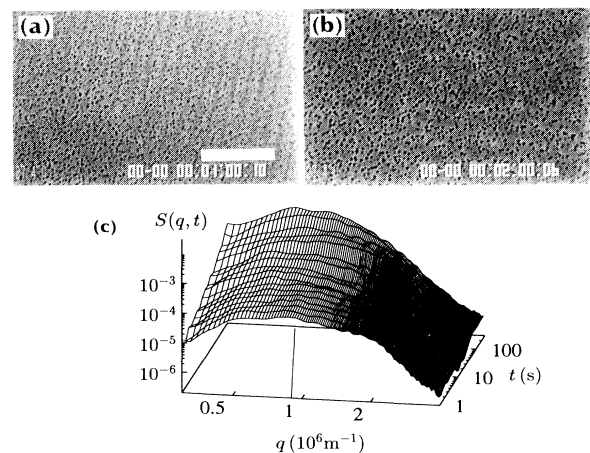


FIG. 2. Phase separation pattern in PS-H/DEM (0.98 wt. % PS). (a) 60 s and (b) 120 s after the quench to  $27.4^{\circ}\text{C}$ . The bar is  $100 \mu\text{m}$  in length. (c) Temporal change in  $S(q, t)$ . Solid line in the  $xy$  plane represents  $q_m \sim t^{-0.1}$ .

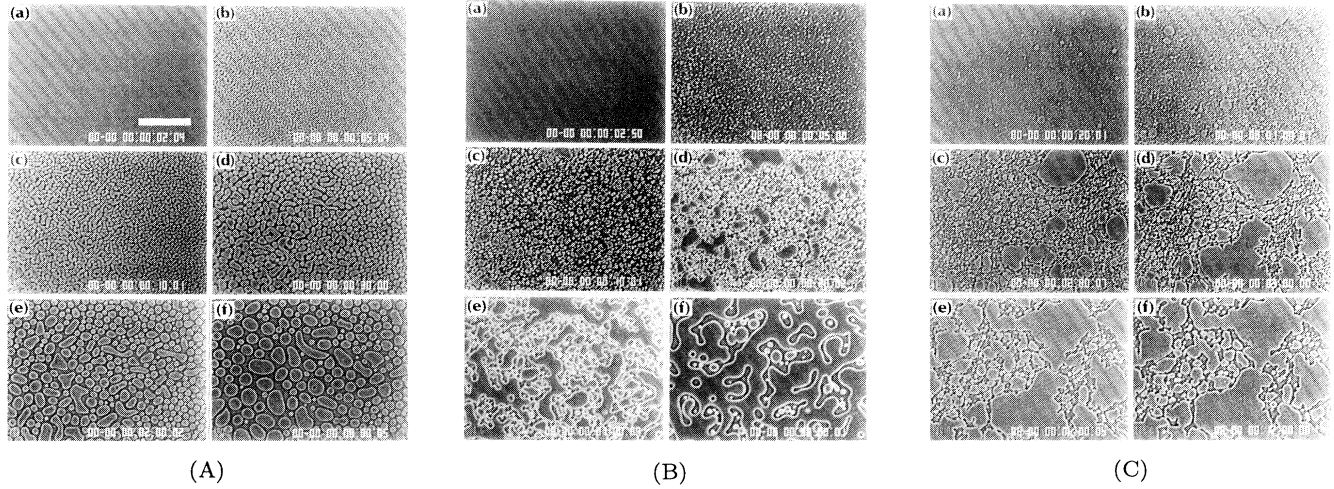


FIG. 3. Pattern evolution during phase separation (A): PS-L/DEM (8.7 wt. % PS); (a) 2 s, (b) 5 s, (c) 10 s, (d) 30 s, (e) 120 s, and (f) 480 s after the quench to 14.5°C. (B): PS-M/DEM (7.0 wt. % PS); (a) 2.5 s, (b) 5 s, (c) 10 s, (d) 20 s, (e) 60 s, and (f) 480 s after the quench to 9.2°C. (C): PS-H/DEM (4.0 wt. % PS); (a) 20 s, (b) 60 s, (c) 120 s, (d) 180 s, (e) 360 s, and (f) 720 s after the quench to 14.8°C. The bar in (A) is 200  $\mu\text{m}$  in length.

3(A)–3(C) likely comes from the difference in the degree of dynamic asymmetry between the two phases which can be characterized by the *dynamic asymmetry parameter*  $p_{\text{da}} = \tau_t^{\text{pr}} / \tau_t^{\text{sr}}$ . Here  $\tau_t^{\text{pr}}$  and  $\tau_t^{\text{sr}}$  are  $\tau_t$  for the polymer-rich and solvent-rich phases, respectively. Since  $p_{\text{da}}$  is proportional to  $N\phi_{\text{pr}}^{3/2}$  for a deep quench,  $p_{\text{da}}$  drastically increases with  $N$  and  $\Delta T$ . Thus the viscoelastic effect becomes significant for large  $N$  or  $\Delta T$ . For shallow quench conditions where  $p_{\text{da}} \sim 1$  (dynamically symmetric cases), it has already been confirmed experimentally that usual spinodal decomposition proceeds in both polymer solutions and polymer mixtures [1,12]. The limited range of  $p_{\text{da}}$  in the previous experiments is the reason why the behavior in these systems has so far been believed to be the same as that in binary liquid mixtures [1].

First we discuss the coarsening dynamics of MDP. The viscoelastic effect should be considered when the characteristic time of the collision (or the contact time)  $\tau_c$  is shorter than or comparable to  $\tau_t$ . Brownian motion of a droplet with mass  $m$  is characterized by a randomly varying thermal velocity of magnitude  $\langle v \rangle \sim (k_B T / m)^{1/2}$  and

duration  $\tau_r \sim m D_R / k_B T$  ( $D_R$ : the diffusion constant of a droplet with radius  $R$ ). Thus  $\tau_c$  should satisfy the relation  $r_0 / \langle v \rangle < \tau_c < r_0^2 / D_R$ , where  $r_0$  is the range of interaction. Next,  $\tau_t$  in a polymer-rich droplet can roughly be estimated as  $\tau_t \sim a^2 N^3 \phi_{\text{pr}}^{3/2} / D_1$  ( $a$  is the length of a unit monomer and  $D_1$  is the diffusion constant of a monomer) [13]. For large  $N$  and  $\phi_{\text{pr}}$ ,  $\tau_t$  could be longer than  $\tau_c$ . For such a case, a droplet usually behaves as an *elastic body* on the collision time scale. This viscoelastic effect is probably responsible for the unusual slow coarsening ( $\alpha \leq 0.1$ ) and the unusual dependence of the coarsening rate on  $\Delta T$ . Since  $\tau_t$  is strongly dependent on  $N$  and  $\phi_{\text{pr}}$ , it is natural that this phase exists only in a polymer solution having large  $N$  for large  $\Delta T$ . With an increase in  $\tau_t / \tau_c$ , the coarsening rate becomes slower and finally MDP might be kinetically stabilized for  $\tau_t \gg \tau_c$  [10].

Next we consider the pattern evolution observed in Figs. 3(B) and 3(C). In the initial stage, the viscoelastic effect becomes more important with an increase in  $\phi$  through the dependence of  $\sigma^{(n)}$  on  $\phi$ :  $\sigma^{(n)}$  is likely proportional to  $-\phi^{5/2} N^3$  for  $\phi > \phi^*$ . In this initial stage the phase-separated structure seems to be frozen for a while, and after a certain incubation time holes of solvent emerge (see Fig. 3(C) [(b) and (c)]). This can also be confirmed from the transitional behavior in Fig. 4. This hole formation process looks similar to the nucleation and growth in the metastable state: The parts where  $\nabla \cdot \sigma^{(n)}$  has locally relaxed might promote the nucleation of solvent-rich droplets. It should be noted that the incubation time is much longer for Fig. 3(C) ( $\sim 20$  s) than for Fig. 3(B) ( $\sim 3$  s). This clearly indicates that viscoelasticity is responsible for this unusual frozen state. The origin of the frozen state could be explained as follows: The self-induced velocity field caused by phase sep-

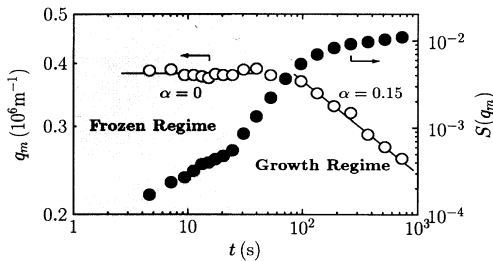


FIG. 4. Temporal change in  $q_m$  ( $\circ$ ) and  $S(q_m)$  ( $\bullet$ ) for PS-H/DEM (4.0 wt. %) quenched into 14.8°C [see Fig. 3(C)].

aration creates the stress field, which transiently shifts the phase diagram. This apparent phase diagram likely corresponds to a virtual free energy including the contribution from  $\sigma^{(n)}$  (see the first equation), which is estimated as  $g(\phi, t) = f(\phi) + k(t)\phi^{5/2}N^3$  [ $k(t)$ : a coupling factor decreasing with  $t$ ]. This physical picture can be easily understood if we consider the extreme situation such as gels or elastic solids [14], in which the Hamiltonian directly includes the elastic effect. Although it is well known that the external stress field shifts the phase diagram [15], this kind of viscoelastic effect due to the self-induced, internal velocity field has never been considered. Thus further study is necessary to clarify the effect.

In the initial kinetic regime the asymmetry in the molecular dynamics plays a more important role than the composition asymmetry, although the final state is dominated by the composition asymmetry. In Fig. 1 we schematically indicate both the symmetric composition determined by the kinetically deformed, apparent phase diagram,  $g(\phi, t)$ , and that determined by the thermodynamic phase diagram,  $f(\phi)$ . This gap between the two kinds of symmetry, namely *dynamic and static symmetry*, is likely responsible for the unusual temporal change in the concentration distribution even after the formation of a sharp interface. In the right-hand side of the *kinetic-symmetry* line, the polymer-rich phase appears in the continuous, matrix phase in the initial stage. In its left-hand side, on the other hand, the polymer-rich phase appears as a droplet phase and MDP is formed. Between the *kinetic- and static-symmetry* lines, the polymer-rich phase appears as the major (matrix) phase in the initial stage and then it transforms into the minority (droplet) phase as in Figs. 3(B) and 3(C).

After the frozen regime, the characteristic domain size commonly grows as  $t^{0.15}$ . This coarsening process is considerably slower than that for usual binary fluids [1] probably because the pattern evolution is dominated by the slow dynamics of the polymer-rich, viscoelastic phase. In the late stage the polymer-rich, matrix phase shrinks, discharging the solvent, reflecting the change in  $g(\phi, t)$ , and adopts the unusual networklike structure (NP). A tensile force acts along the thin part of the matrix since the elastic contribution from  $\sigma^{(n)}$  should be dominant because of the large deformation rate. If the elongated part is not thick enough to support the tension, it splits in two and relaxes to the force-free shape. Locally, NP has a geometrical characteristic unique to 2D systems: the angle between branches approximates  $120^\circ$  in many places, reflecting the force-balance condition. In the very late stage, on the other hand, the stress field is mostly relaxed, reflecting the decay of the deformation rate and instead the  $\nabla\phi$  term in  $\pi$  has the most significant contribution. Thus the interface tension governs the pattern evolution in this stage and the domain starts to become spherical. The morphological transition from NP

to round-interface pattern in the late stage [Figs. 3(B) and 3(C)] can be explained by the above physical picture of viscoelastic relaxation.

In summary, we have found unusual *viscoelastic spinodal decomposition* for ideal polymer/liquid mixtures. The behavior is strongly dependent on the asymmetry in molecular dynamics between the two phase-separated phases. The stress field can be strongly coupled with the order parameter through the velocity field for large  $p_{da}$ . The order parameter is no longer only the slow variable of the system. The concept of the *dynamic symmetry* is introduced in addition to the static, composition symmetry. Dynamically asymmetric polymer mixtures do not belong to the dynamic universality class called *model H*, and they should be classified into a new universality class. Similar phenomena could be observed for any mixture, one of whose components has intrinsic slow dynamics (e.g., complex fluids and mixtures, one of whose component is near glass transition).

This work was partly supported by a Grant-in-Aid from the Ministry of Education, Science, and Culture, Japan.

- 
- [1] J.D. Gunton, M. San Miguel, and P. Sahni, in *Phase Transition and Critical Phenomena*, edited by C. Domb and J.H. Lebowitz, (Academic, London, 1983), Vol. 8.
  - [2] P.C. Hohenberg and B.I. Halperin, *Rev. Mod. Phys.* **49**, 435 (1976).
  - [3] M.A. Kotnis and M. Muthukumar, *Macromolecules* **25**, 1716 (1992).
  - [4] F. Brochard and P.G. de Gennes, *Macromolecules* **10**, 1157 (1977); F. Brochard, *J. Phys. (Paris)* **44**, 39 (1983).
  - [5] E. Helfand and G.H. Fredrickson, *Phys. Rev. Lett.* **62**, 2648 (1989).
  - [6] A. Onuki, *J. Phys. Soc. Jpn.* **59**, 3423 (1990); *ibid.* **10**, 3427 (1990); *J. Phys. II (France)* **2**, 1505 (1992).
  - [7] M. Doi and A. Onuki, *J. Phys. II (France)* **2**, 1631 (1992).
  - [8] K. Hamano *et al.*, *Phys. Rev. A* **20**, 1135 (1979).
  - [9] H. Tanaka *et al.*, *J. Appl. Phys.* **59**, 3627 (1986); **65**, 4480 (1989).
  - [10] H. Tanaka, *Macromolecules* **25**, 6377 (1992).
  - [11] Such behavior could be caused by wetting [see, e.g., J. Bodensohn and W.I. Goldberg, *Phys. Rev. A* **46**, 5084 (1992) and H. Tanaka, *Phys. Rev. Lett.* **70**, 2770 (1993)]. However, the phase separation observed here is probably not affected by wetting phenomena since three-dimensional phase separation in a thick capillary with a radius of  $100\ \mu\text{m}$  was essentially the same as the networklike phase separation between glass plates.
  - [12] See e.g., N. Kuwahara *et al.*, *Phys. Rev. A* **25**, 3449 (1982).
  - [13] P.G. de Gennes, *Scaling Concepts in Polymer Physics* (Cornell Univ. Press, Ithaca, 1979).
  - [14] A. Onuki and H. Nishimori, *Phys. Rev. B* **43**, 13649 (1991).
  - [15] See e.g., J.R. Schmidt and B.A. Wolf, *Colloid. Polym. Sci.* **257**, 1188 (1979).

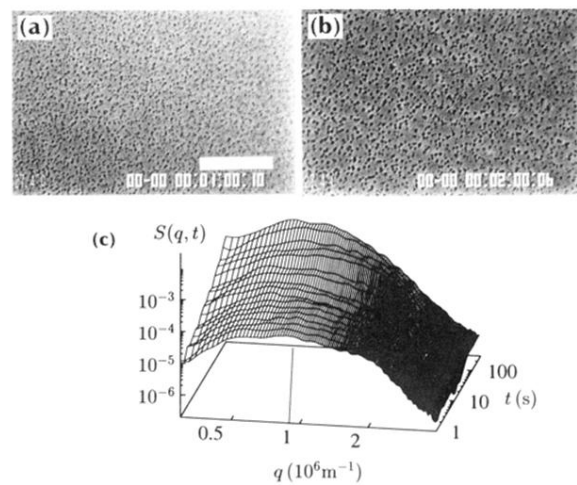


FIG. 2. Phase separation pattern in PS-H/DEM (0.98 wt. % PS). (a) 60 s and (b) 120 s after the quench to 27.4°C. The bar is 100  $\mu\text{m}$  in length. (c) Temporal change in  $S(q, t)$ . Solid line in the  $xy$  plane represents  $q_m \sim t^{-0.1}$ .

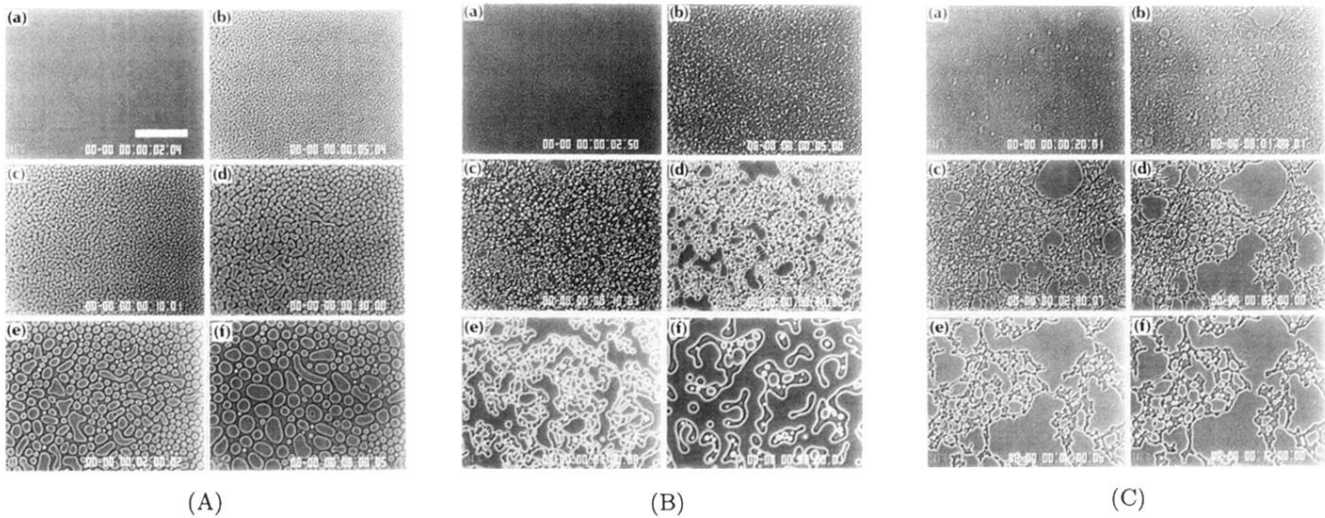


FIG. 3. Pattern evolution during phase separation (A): PS-L/DEM (8.7 wt. % PS); (a) 2 s, (b) 5 s, (c) 10 s, (d) 30 s, (e) 120 s, and (f) 480 s after the quench to 14.5°C. (B): PS-M/DEM (7.0 wt. % PS); (a) 2.5 s, (b) 5 s, (c) 10 s, (d) 20 s, (e) 60 s, and (f) 480 s after the quench to 9.2°C. (C): PS-H/DEM (4.0 wt. % PS); (a) 20 s, (b) 60 s, (c) 120 s, (d) 180 s, (e) 360 s, and (f) 720 s after the quench to 14.8°C. The bar in (A) is 200  $\mu\text{m}$  in length.

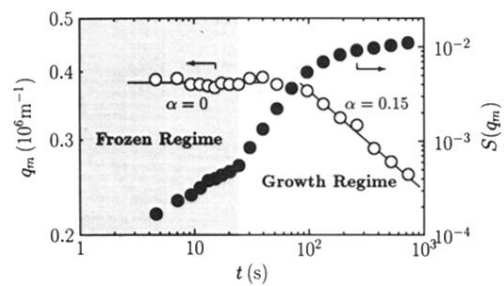


FIG. 4. Temporal change in  $q_m$  ( $\circ$ ) and  $S(q_m)$  ( $\bullet$ ) for PS-H/DEM (4.0 wt. %) quenched into  $14.8^\circ\text{C}$  [see Fig. 3(C)].